

Kinetics of spatial distribution of electron-hole drops

N. V. Zamkovets, N. N. Sibel'din, V. B. Stopachinskiĭ, and V. A. Tsvetkov

P. N. Lebedev Physics Institute, USSR Academy of Sciences

(Submitted 5 October 1977)

Zh. Eksp. Teor. Fiz. **74**, 1147–1158 (March 1978)

Absorption, scattering, and luminescence methods are used to investigate the kinetics of the spatial distribution of electron-hole drops (EHD) in germanium under surface pulsed excitation. It is shown that the drop cloud moves within a time of several microseconds from the illuminated surface into the interior of the crystal, and then stops at a distance 2–3.5 mm from the surface. This distance increases with increasing excitation density and with decreasing temperature, and depends on the geometry of the experiment. Thus, even in the case of surface excitation, the EHD spends the greater part of its existence inside the sample volume. The experimental results are interpreted on the basis of the theory of dragging of the drops by the phonon wind [V. S. Bagaev *et al.*, *Sov. Phys. JETP* **43**, 362 (1976); V. L. Keldysh, *JETP Lett.* **23**, 86 (1976)].

PACS numbers: 71.35.+z, 78.55.Hx, 71.38.+i

The influence of the dragging of electron-hole drops (EHD) by nonequilibrium phonons produced in the course of thermalization and nonradiative recombination of nonequilibrium carriers on the spatial distribution of the drops was considered theoretically in^[1,2]. The dragging effect has made it possible to explain a large number of the results of measurements of the EHD diffusion coefficient. Bagaev *et al.*^[1] cite also results of experiments on the observation of the motion of EHD under the influence of phonon wind with stationary excitation of the nonequilibrium carriers; these results confirm the conclusions of the theory. The use of pulsed excitation for the study of this phenomenon is of particular interest, for in this case it is possible to trace the evolution of the spatial distribution in time, and deduce on its basis the causes and the mechanism of the EHD motion. Keldysh^[2] considered two possibilities: dispersal of large volumes of the electron-hole liquid in the form of minute droplets, and expansion of the droplet cloud as a result of the mutual repulsion of the EHD.

Under pulsed excitation, the dragging of the EHD by the phonon wind was first investigated in^[3], in^[4] this effect was investigated under uniaxial compression of the crystal, and a microwave method was used in^[5] to register the motion of the EHD. The peculiarities of the experimental procedures used in these studies has not made it possible, however, to obtain information on the spatial distribution of the EHD.

It was observed in^[6] that in the case of surface pulsed excitation the EHD fill a narrow layer that moves away from the illuminated surface. This fact has not been satisfactorily explained to this day. To interpret it, a hypothesis advanced that the EHD moves ballistically,^[7] but this hypothesis does not seem to be sufficiently well founded, since an unrealistically long EHD momentum relaxation time is required to explain the experimental data. The assumption of a phonon wind that is produced in the EHD themselves can likewise not offer at present a final explanation of the formation of the drop layer observed in^[6].

We have previously shown^[8] that there are two stages

of EHD motion: "fast," wherein the drop layer is produced, and "slow," due to the mutual repulsion of the EHD.^[1] In the present article we present the results of an investigation of the fast phase of drop motion in the case of surface pulsed excitation. In accordance with^[6], after the exciting pulse was turned on, formation of an EHD layer is observed, moving from the excited surface into the interior of the crystal in a time interval that is short compared with the lifetime of the drops. The character of the change of the spatial distribution of the EHD in time did not depend on the excitation level or on the temperature. However, the distance negotiated by the drops during the time of their motion increased with increasing excitation level and with decreasing temperature.

Measurements of the kinetics of the total number of nonequilibrium carriers have shown that the layer moves so long as fast nonradiative recombination of the nonequilibrium carriers takes place. The layer motion is well described by the phonon-wind theory,^[1,2] but the mechanism of phonon generation and the states of the carriers that generate these phonons are not clear at present.

EXPERIMENTAL PROCEDURE

The measurements were performed with the setup described in detail in^[9]. The excitation source was a pulsed copper-vapor laser (emission wavelength 0.51 μm , pulse duration ~ 10 nsec, repetition frequency ~ 5 kHz, maximum energy in pulse ~ 120 erg). The exciting radiation was focused on the lateral surface of the sample into a spot of specified dimension and shape. The excitation level was varied with calibrated neutral light filters.

We investigated the spatial distribution of the absorption and scattering of probing radiation of wavelength 3.39 μm . The probe source was a cw Ne-He laser. Its beam was focused on the front (broad) face of the sample at a given distance x from the excited surface (Fig. 1). In the measurement of the absorption, the probing radiation passing through the sample was focused with a

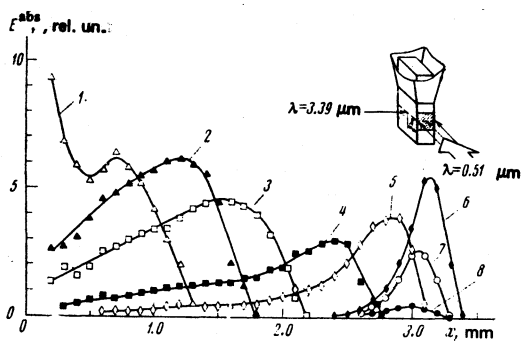


FIG. 1. Spatial distribution of absorption at various instants of time t , μsec : 1-0; 2-0.5; 3-1.0; 4-2.0; 5-3.0; 6-7.0; 7-30; 8-75. Upper right corner—experimental setup, $T=1.7\text{K}$.

quartz lens on a Ge: Au photoreceiver cooled with liquid nitrogen. In the measurement of the scattering, the angular distribution of the probing radiation scattered by the EHD was recorded with a goniometer. The scattered light was preamplified by an optical quantum amplifier and then recorded by the very same photoreceiver. The time resolution of the system for the registration of the absorption and the scattering was not worse than $0.5 \mu\text{sec}$, and the operating time did not exceed $0.2 \mu\text{sec}$.

The spatial distribution of the EHD recombination radiation was measured by varying the distance x from the exciting surface to the image of the MDR-2 monochromator slit on the sample. The monochromator was tuned to the maximum of the drop line. The recombination radiation was registered with a germanium photodiode.

The measurements were made on mechanically polished germanium samples with residual-impurity concentration less than 10^{12}cm^{-3} . The samples measured $15 \times 5 \times 3 \text{mm}$ and were sealed into the helium volume of the cryostat in such a way that the working half of the sample was in vacuum.

RESULTS AND DISCUSSION

Figure 1 shows the spatial distribution of the absorption (spatial resolution $\sim 300 \mu\text{m}$) at different instants of time, reckoned from the instant of operation of the registration system ($t=0$). These data were obtained at a temperature 1.7K and a maximum excitation level in a planar geometry of the experiment (the dimensions of the exciting spot $4 \times 3 \text{mm}$ exceeded the distance x from the excited surface; the motion could in this case be regarded approximately as uniform. Assuming that the absorption signal is proportional to the number of nonequilibrium carriers in the probing beam, the distribution of the absorption over the sample is a reflection of the spatial distribution of the nonequilibrium carriers. It is seen from Fig. 1 that even at the initial instant of time the nonequilibrium carriers fill in the sample a volume of thickness $x \approx 1.3 \text{mm}$. In the course of time the leading front of the cloud of nonequilibrium carriers moves into the interior of the crystal, and a long tail is

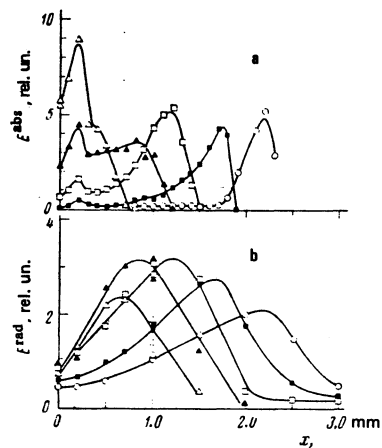


FIG. 2. Spatial distribution of the absorption (a) and of the intensity of the EHD recombination radiation (b) at various instants of time t , μsec : 1-0(Δ); 2-0.5(\blacktriangle); 3-1.0(\square); 4-2.0(\blacksquare); 5-7.0(\circ); $T=1.7\text{K}$.

formed on the trailing edge. By the instant $t=7 \mu\text{sec}$ the cloud stops, and its trailing edge is drawn towards the leading one, as is evidenced by a certain increase of the absorption signal at the instant of stopping of the cloud, i.e., the carrier density in the cloud increases. Subsequently, owing to carrier recombination, the absorption signal decreases. We note that the cloud does not expand after it is stopped. This circumstance was carefully verified since it is important for the numerical estimate of the constant of the repulsion interaction of the EHD (see below). The described picture of the evolution of the spatial distribution agrees in general outline with that observed in^[6].

To calculate the nature of the state of the nonequilibrium carriers, we measured the spatial distribution of the recombination radiation of the EHD and of the scattering of the sounding radiation. Figure 2 shows the spatial distribution of the absorption (Fig. 2a, spatial resolution $\sim 200 \mu\text{m}$) and of the intensity of the EHD recombination radiation (Fig. 2b, spatial resolution $\sim 500 \mu\text{m}$), obtained under identical experimental conditions. At $t \geq 1 \mu\text{sec}$, a correlation is observed between the positions of the maxima of the absorption signals and of the recombination radiation of the EHD. At t equal to 0 and $0.5 \mu\text{sec}$, however, the maximum of the drop radiation is on the leading front of the cloud of the nonequilibrium carriers, i.e., the EHD is formed mainly on the edge of the cloud where the concentration of the nonequilibrium carriers is relatively small. In the course of time, the EHD layer produced in this manner moves into the interior of the crystal, and the concentration of the nonequilibrium carriers near the illuminated surface of the sample decreases rapidly, as is seen from Figs. 1 and 2a.

We emphasize that despite the use of surface excitation, the EHD spends the greater part of its lifetime in the interior of the crystal at an appreciable distance from the excited surface. The measurements of the kinetics of the spatial distribution of the scattering signal confirm the described picture of the formation and motion of the EHD layer.

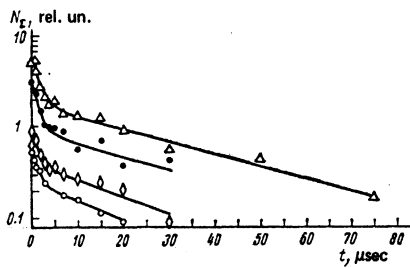


FIG. 3. Kinetics of total number of nonequilibrium carriers N_E at $T=1.7$ K and at various excitation levels: $I/I_{\max}=1(\Delta)$, $0.63(\bullet)$, $0.45(\diamond)$ and $0.36(\square)$.

The experiments performed in spherical (focusing into a point) and cylindrical (focusing into a narrow strip parallel to the probing beam) excitation geometries have shown that in these cases there is produced either a spherical or a cylindrical EHD layer that moves for some time away from the excitation region into the interior of the crystal.

When the excitation intensity and the crystal temperature change, the character of the spatial distribution and of the EHD motion do not change. However, with increasing excitation level and with decreasing temperature, the velocity of the EHD and the maximum distance covered by it increase.

We shall discuss hereafter results obtained at a planar excitation geometry, since in this case the reduction of the results and their comparison with the theory are simplest, although the same qualitative conclusions can be drawn from experiments performed in spherical or cylindrical geometry. Figs. 3 and 4 show the time dependences of the total number of nonequilibrium carriers in the sample, N_E , at various excitation levels and at temperatures 1.7 and 4.2 K. The values of N_E at different instants of time were obtained by graphical integration of the plots of the spatial distribution of the absorption, similar to those shown in Figs. 1 and 2a, with respect to the coordinate x . The plots of N_E against t show two sections: a fast decrease of N_E with a time constant $\tau_{ph} \approx 2-3$ μsec , which gives way to an exponential decrease with a lifetime $\tau_0 \approx 32$ μsec ($T=1.7$ K) or to a nonexponential decrease of the total number of carriers with time at the temperature 4.2 K. The exponen-

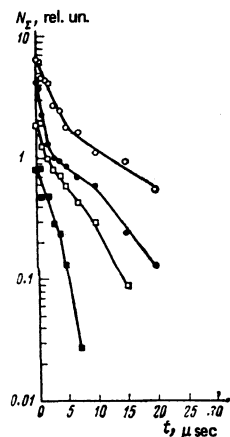


FIG. 4. Kinetics of total number of nonequilibrium carriers at $T=4.2$ and at different excitation levels: $I/I_{\max}=1(\circ)$, $0.79(\square)$, $0.57(\triangle)$ and $0.28(\diamond)$.

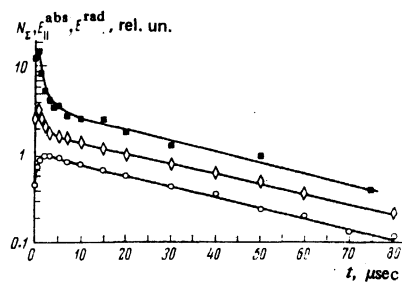


FIG. 5. Kinetics of $N_E(\blacksquare)$, $E_{\text{rad}}^{\text{abs}}(\diamond)$ and of the integrated (over the sample volume) intensity of EHD recombination radiation $E_{\text{rad}}^{\text{rad}}(\circ)$ at $T=1.7$ K.

tial with $\tau_0 \approx 32$ μsec corresponds to recombination of nonequilibrium carriers bound in the EHD.^[10-12] At 4.2 K, owing to the strong evaporation of the EHD, the recombination proceeds mainly through a gas phase,^[10-14] and the rate of the recombination increases with decreasing excitation level,^[13-14] as is clearly seen from the curves of Fig. 4 at large t .

From a comparison of the upper curve of Fig. 3 with the evolution of the spatial distribution of the nonequilibrium carriers (Fig. 1) we can conclude that the EHD move inside the crystal until a rapid decrease of the total number of the nonequilibrium carriers N_E is observed.

In this case there is no fast component in the kinetics of the EHD recombination radiation (the $E_{\text{rad}}^{\text{rad}}$ curve on Fig. 5). These data differ from the results of^[5, 14], where drop motion and fast kinetics were simultaneously observed in the luminescence of the EHD. Fast kinetics in the EHD luminescence was observed by us (just as in^[14]) for thin samples at much higher excitation levels then used in the cited experiments. It is possible that the appearance of a fast decrease in the kinetics of the recombination radiation of the EHD is the consequence of the drop motion, as noted in^[13, 14], whereas the cause of the motion is apparently the interaction of the EHD with the intense fluxes of the nonequilibrium phonons, whose generation rate during the fast decrease of N_E is quite large.

The phonon generation mechanism and the nature of the state of the carriers that emit these phonons are at present not completely clear. It is possible that the phonons are produced in nonradiative recombination of nonequilibrium carriers that are not bound in EHD, or as a result of fast nonradiative (e.g., on the crystal surface) recombination of the drops, with a lifetime $\tau_{ph} \approx 2-3$ μsec . In any case, however, in nonradiative recombination the excitation energy of the crystal goes over in final analysis entirely to the phonons.

We emphasize that we are dealing in this case with the motion of an EHD layer produced on the leading front of a cloud of nonequilibrium carriers (Fig. 2) under the influence of the phonon wind that arises in the case of fast recombination of the carrier on the trailing edge of the cloud near the excited surface (Figs. 1 and 2a). This is precisely the motion that we named "fast" in^[8]. The term "fast" phase of motion characterizes in this case not the motion velocity, but the fast decrease of

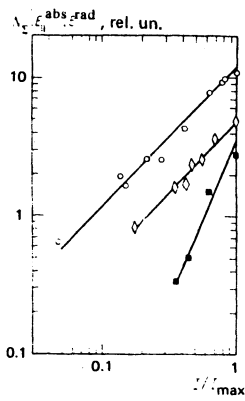


FIG. 6. Plots of N_{Σ} (■), $E_{||}^{\text{abs}}$ (◇) and E^{rad} (○) against the excitation level I . $T=1.7\text{K}$, $t=2$.

the total number of nonequilibrium carriers, in the course of which a directed phonon flux is produced, and a relatively short duration of the motion compared with the lifetime of the drops. On the contrary, "slow" motion of drops^[8] is produced by the forces of their mutual repulsion, which is due to the generation of phonons by the drops themselves as a result of Auger recombination of the carriers bound in the EHD^[1, 2]; in this case the rate of phonon generation is relatively small (the carrier lifetime in the EHD is $\tau_0 \gg \tau_{ph}$), and the duration of the drop motion can exceed τ_0 ^[8].

Before we proceed to the analysis of the results from the point of view of the theory of phonon wind, we note one more circumstance, which is evident from Fig. 3, namely the faster-than-linear dependence of N_{Σ} on the excitation level I (Fig. 6). The plot of N_{Σ} against I shown in Fig. 6 was obtained 2 μsec after the excitation pulse, but the dependence is of the same form for any instant of time t . The integrated (over the sample volume) intensity of the EHD recombination radiation increases here linearly with increasing excitation level (Fig. 6).

The total number of nonequilibrium carriers in the sample can be measured directly, without going through the stage of graphic integration of the curves of the spatial distributions of the absorption which are shown in Fig. 1. To this end, the probing beam should propagate along the x axis. The integration with respect to x is then carried out automatically in the course of the measurement and the absorption signal should be proportional to the total number of nonequilibrium carriers. The results of such an experiment are shown in Figs. 5 and 6 (the $E_{||}^{\text{abs}}$ curves). In the kinetics of the $E_{||}^{\text{abs}}$ signal one observes a section with a rapid decrease at small t . At large t , the decrease of $E_{||}^{\text{abs}}$ in the course of time has the same time constant $\tau_0 = 32 \mu\text{sec}$ as the decreases of N_{Σ} and E^{rad} (Fig. 5). In contrast to the dependence of N_{Σ} on I , however, $E_{||}^{\text{abs}}$ increases linearly with the excitation level (Fig. 6). At the present time we have no satisfactory explanation of this fact. It is possible that the superlinear dependence of N_{Σ} on I is determined by the contribution made to the absorption by the carriers that are concentrated near the sample surfaces parallel to the x axis, and these carriers are not registered when $E_{||}^{\text{abs}}$ is measured. In such a case the distribution of the absorption over the sample (Figs. 1 and 2a) accounts only qualitatively for the char-

acter of the spatial distribution of the nonequilibrium carriers. However, the position of the leading front of the drop cloud at each instant of time can be exactly determined from the spatial distribution of the absorption, a fact of particular importance in the subsequent analysis.

It must be noted that many workers^[5, 15, 16] have observed a threshold-like appearance and an abrupt growth of microwave absorption for a linear increase of the intensity of the EHD recombination radiation with increasing excitation. These results have not yet been incontrovertibly explained. It is possible that the faster-than-linear growth of N_{Σ} and of the microwave absorption have one and the same nature.

Let us see now how the spatial distribution of the EHD should change with time under the influence of phonon wind. If we have at the instant of time t_0 an infinite flat layer of thickness $x(t_0)$, homogeneously filled with drops, then in the course of time, as a result of the dragging of the drops by the phonons produced in the course of the nonradiative recombination of the carriers bound in the EHD, the layer thickness will increase, and the coordinate of its boundary varies like^[2]

$$x(t) = x(t_0) \left[1 + 2\pi\rho^2 \frac{\tau_p \tau_0}{n_0^2 m^* x(t_0)} \Delta N_{\Sigma}(t) \right], \quad (1)$$

the distribution of the drops over the volume of the layer remaining uniform.

In Eq. (1), τ_p is the momentum relaxation time of the carriers in the EHD, τ_0 is the lifetime of the carriers in the liquid phase, n_0 is their density, m^* is the effective mass of the electron-hole pair, $\Delta N_{\Sigma}(t)$ is the number of carriers in the liquid phase per unit layer area that recombine during the time from t_0 to t , and ρ is the constant of the repulsion interaction of the EHD and its explicit form is given in^[2]. In our preceding paper^[1] we considered two mechanisms of interaction between nonequilibrium phonons and EHD, namely phonon absorption and phonon scattering. It appears that the "phonon wind" is determined mainly by the phonon absorption process, and the theoretical estimate given in^[1] for the scattering probability of the short-wave phonons is greatly overestimated. At the same time, an appreciable fraction of the energy (1–10%) of the Auger electrons goes to heating the carriers in the EHD and is reradiated in the form of long-wave ($k \leq 2k_F$) phonons.^[2] By the same token, the absorption process becomes predominant.

Thus, the theory cannot explain the formation of the EHD layer if the initial spatial distribution was homogeneous. However, if such a layer was in fact produced, then its subsequent motion should be described by expression (1) in which $\Delta N_{\Sigma}(t)$ should be taken to mean the total number of carriers, per unit area, whose energy was released in the form of phonons during the time from t_0 to t .

It is seen from (1) that the distance covered by the leading front of the drop cloud in the time interval $t - t_0$ is

$$\Delta x(t) = x(t) - x(t_0) = 2\pi\rho^2 \frac{\tau_p \tau_0}{n_0^2 m^*} \Delta N_{\Sigma}(t), \quad (2)$$

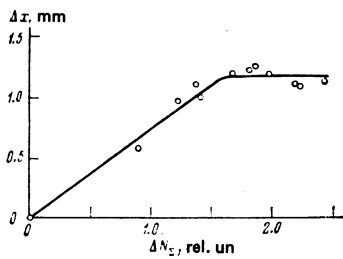


FIG. 7. Plot of the distance Δx traversed by the drops against the number of recombined carriers ΔN_{Σ} ($T=1.7\text{K}$; $I=I_{\max} \approx 120$).

i.e., it is proportional to $\Delta N_{\Sigma}(t)$. Figure 7 shows an experimental plot of Δx against ΔN_{Σ} . To construct this plot, the values of Δx were taken from Fig. 1, and the corresponding values $\Delta N_{\Sigma} = N_{\Sigma}(t_0) - N_{\Sigma}(t)$ were taken from Fig. 3, where the points marked on the last figure correspond to the linear section of the dependence of V on x (Fig. 8b). It is seen from Fig. 7 that up to the time that the drops are stopped the growth of Δx is described by expression (2). This means that under the conditions of our experiments a planar excitation geometry is indeed realized for the excitation and motion of the drops, for otherwise the dependence of Δx on ΔN_{Σ} would be more complicated.^[2, 8]

Differentiating (1) with respect to the time t , we obtain expressions that describe the time dependences of the drop velocity on the leading front of the cloud:

$$V = \frac{dx}{dt} = V_0 \exp\left(-\frac{t-t_0}{\tau_{ph}}\right) \quad (3)$$

and the dependence on the coordinate of the leading front $x(t)$:

$$V = V_0 - \frac{x(t) - x(t_0)}{\tau_{ph}}, \quad (4)$$

where

$$V_0 = 2\pi\rho^2 \frac{\tau_p \tau_0 N_{\Sigma}(t_0)}{n_0^2 m^2 \tau_{ph}} \quad (5)$$

is the initial (at the instant of time t_0 at the point $x(t_0)$) motion velocity. In the derivation of (3) and (4) it was assumed that $N_{\Sigma}(t)$ varies with time like

$$N_{\Sigma}(t) = N_{\Sigma}(t_0) \exp[-(t-t_0)/\tau_p]. \quad (6)$$

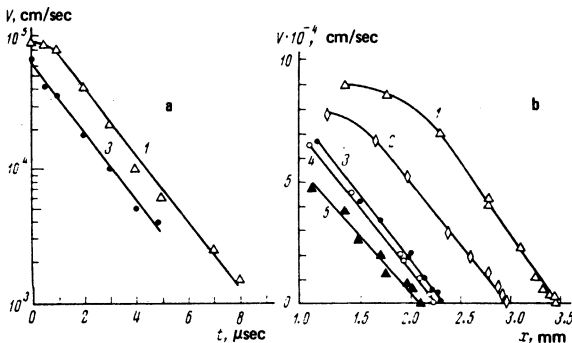


FIG. 8. Plots of the velocity of the leading front of the drop cloud against the time (a) and the coordinate (b) 1, 2, 3, 4 - $T=1.7\text{K}$; 1 - $I/I_{\max}=1.0$; 2 - 0.63; 3 - 0.45; 4 - 0.36; 5 - $T=4.2\text{K}$, $I/I_{\max}=1.0$ ($I_{\max} \approx 120\text{erg/pulse}$).

Here τ_{ph} is the time constant of the rapid decrease of the total number of the nonequilibrium carriers (see Figs. 3 and 4).

The dependences of the instantaneous velocity of drop motion on the time and on the coordinate are shown in Fig. 8. The instantaneous velocity was taken to be the velocity averaged over a time interval much larger than τ_p but small compared with the total time of motion. At not too high motion velocities, the experimental results are well described by expressions (3) and (4). From the slopes of the lines on Fig. 8 we can obtain τ_{ph} , which turns out to be $\tau_{ph} \approx 1.8 \mu\text{sec}$ at $T=1.7\text{K}$, in satisfactory agreement with the data of Fig. 3. The deviation, observed at large V , from the relations predicted by (3) and (4) should not be surprising, since expressions (1)–(4) were written out under the assumption that V is much less than the speed of sound (s) in the crystal.

When the temperature was increased from 1.7 to 4.2 K, the velocity of the EHD decreased by an approximate factor of 3 (the ratio of the velocities was taken at the instant $t=1 \mu\text{sec}$, which corresponds to the linear section of the velocity plot on Fig. 8b). This means that the drop mobility has decreased by the same factor, if we assume that τ_{ph} and ρ do not change with temperature.

Figure 9 shows the dependence of the instantaneous velocity of the drop motion on the excitation intensity. This figure shows the velocity values taken for one and the same instant of time $t=2 \mu\text{sec}$ on the linear sections of the curves of Fig. 8b, i.e., when the experimental data are described by expression (4). The linear growth of the velocity of the drops follows from expressions (3) and (5), if $N_{\Sigma}(t_0)$ is proportional to the excitation level I . This result agrees with the linear dependence of E^{abs} on I (Fig. 6).

A faster-than-linear dependence of the drop velocity on the excitation intensity was observed in^[5]. There, however, the quantity measured was the average velocity, which can be seen from (3) to depend not only on $N_{\Sigma}(t_0)$ but also on the time of flight of the drops from the point of their formation to the measurement time, and the time of flight decreases with increasing excitation intensity. In addition, they observed a somewhat larger ($\sim 2 \times 10^5 \text{ cm/sec}$) drop velocity than the maximum instantaneous velocity observed in our experiments ($\sim 9 \times 10^4 \text{ cm/sec}$). This discrepancy is apparently due to the fact that even at $t=0$ the nonequilibrium carriers fill a layer of thickness $x(0) \sim 1\text{mm}$ (Fig. 1). Therefore

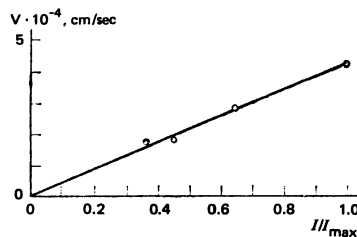


FIG. 9. Dependence of drop velocity on the excitation intensity ($T=1.7\text{K}$; $t=2\mu\text{sec}$).

if we calculate, as was done in^[5], the average velocity from the formula $V_{av} = x(t)/t$, then we obtain from the data of Fig. 1, say for $t = 0.5 \mu\text{sec}$, $V_{av} \approx 3.6 \times 10^5 \text{ cm/sec}$, which even exceeds the value cited in^[5], even though the instantaneous velocity of the drop motion at $t = 0$ amounts to $9 \times 10^4 \text{ cm/sec}$ (Fig. 8). The values of the initial EHD velocity cited in^[6], which exceed the speed of sound, were apparently obtained by extrapolating the plot of the velocity to the point $x = 0$, which is not justified, as seen from Fig. 8.

What remains unclear is the question of the spatial distribution of the nonequilibrium carriers and the EHD at the instant of time $t = 0$. During the time $\sim 0.2 \mu\text{sec}$ the carriers go off to a distance $\sim 1 \text{ mm}$ (Figs. 1 and 2) from the crystal surface excited by the light. To this end, they must move with an average velocity of the order of the speed of sound, or even faster. If the motion is by diffusion, then to obtain a motion with such a velocity the carrier diffusion coefficient must exceed by about two orders of magnitude the exciton diffusion coefficient, which is rather unlikely. It is possible that the carriers are dragged over this distance by the phonon wind produced when they are thermalized. When the carriers are cooled, a powerful flux of phonon energy is produced, exceeding by several orders of magnitude the energy flux responsible for the further motion of the EHD. Therefore, notwithstanding the small relative number of the long-wave phonons that interact effectively with the carriers, the dragging effect can become noticeable.

From the point of view of formation of germs of the liquid phase,^[18-20] the predominant formation of the EHD on the leading front of the cloud of nonequilibrium carriers, where the carrier density is relatively small (Fig. 2, $t = 0$), is incomprehensible. It is possible however, that the crystal region near the excited surface is superheated.

As noted in^[1,2], the lack of information on the distribution function of nonequilibrium phonons makes it difficult to obtain a reliable theoretical estimate of the constant ρ of the repulsion interaction of the EHD. The value of ρ was determined experimentally in^[3-8]. Let us estimate it from the data of the present paper. The upper limit of ρ can be obtained by taking into account the fact that, as noted above the drop cloud did not expand after stopping in the interior of the crystal (Fig. 1). However, if the constant ρ is large enough, the repulsion interaction between the drops should cause the layer to expand in accordance with Eq. (1). If the phonon source are the drops themselves, we have

$$\Delta N_x(t) = N_x(t_0) \left[1 - \exp\left(-\frac{t-t_0}{\tau_0}\right) \right] \approx N_x(t_0) \frac{t-t_0}{\tau_0}.$$

Assuming that a layer expansion by $\Delta x = 0.2 \text{ mm}$ at a time $t - t_0 = 10 \mu\text{sec}$ after its stopping would have been reliably registered by us, and putting $n_0 = 2 \times 10^{17} \text{ cm}^{-3}$, $m^* \approx 4 \times 10^{-28} \text{ g}$, $\tau_p = 2 \times 10^{-8} \text{ sec}$ and $N_x(t_0) \approx 2 \times 10^{13} \text{ cm}^{-2}$, we find, using (2), that $\rho > 100 \text{ g}^{1/2} \text{ cm}^{-3/2} \text{ sec}^{-1}$.

The constant ρ can also be calculated from the slope of the line $\Delta x(t)$ as a function of $\Delta N_x(t)$ (Fig. 7); this

yields (at $\tau_0 = 32 \mu\text{sec}$, $\Delta N_x(t) \approx 5 \times 10^{13} \text{ cm}^{-2}$, and $\Delta x = 1.2 \text{ mm}$) $\rho \approx 100 \text{ g}^{1/2} \text{ cm}^{-3/2} \text{ sec}^{-1}$. In addition, ρ can be estimated by using relation (5) and extrapolating the plot of the EHD velocity to the point $t_0 = 0$. The extrapolation yields $V_0 = 1.3 \times 10^5 \text{ cm/sec}$ for the upper curve of Fig. 8a. At $N_x \approx 10^{14} \text{ cm}^{-2}$ and $\tau_{ph} \approx 1.8 \mu\text{sec}$ we obtain $\rho \approx 100 \text{ g}^{1/2} \text{ cm}^{-3/2} \text{ sec}^{-1}$.³⁾ To derive these values of ρ we calculated N_x from the energy in the exciting laser pulse, as was done in^[3,8].

The value of ρ obtained in the present paper agrees well with the data of^[8] and is somewhat smaller than that given in^[3]. The results of^[3], however, were interpreted without taking into account the fast decrease of N_x at small t , so that the value of ρ given in^[3] should be decreased by a factor $(\tau_0/\tau_{ph})^{1/2} \sim 4$. The value of ρ can also be estimated from data obtained in stationary excitation.^[1,2] An appropriate recalculation yields $\rho \approx 40$ ^[1] and $\rho \approx 60 \text{ g}^{1/2} \text{ cm}^{-3/2} \text{ sec}^{-1}$.^[21] It appears that one should not regard as too significant the discrepancies between the results of different measurements of ρ , since the spectrum of the nonequilibrium phonons can vary with the experimental conditions.

In conclusion, we wish to emphasize that some of the results cannot be uniquely interpreted at present. Nevertheless, it can be regarded as established that the "fast" phase of the EHD motion, which was investigated here and is responsible for the EHD spatial distribution, is the result of the dragging of the drops by the phonon wind. The phonon-wind theory also explains well the observed regularities in the motion of the EHD. The mechanism whereby the phonons are generated, and the states of the carriers that emit these phonons, are presently not clear. The question of the nature of the state of the carriers is apparently crucial not only for a complete explanation of the results of the present paper, but also for the understanding of a large group of phenomena that occur at high ($\geq 10^{15} \text{ cm}^{-3}$) concentrations of nonequilibrium carriers.

We are deeply grateful to V. S. Bagaev and L. V. Keldysh for constant interest in the work and for numerous useful discussions, and to I. V. Kavetskaya and T. N. Shvetsova for help with the experiments.

¹⁾It appears that the stage of drop motion in^[3-6] was in fact the fast one.

²⁾This estimate was obtained from the known formulas for the ionization losses of fast particles in matter^[17] by comparing these losses with the losses to the emission of optical phonons.

³⁾The last two estimates of ρ can, generally speaking, differ from the first estimate, since the spectra of the phonons emitted in the case of the above-described fast nonradiative recombination of the nonequilibrium carrier and in the case of Auger recombination of the carriers bound in the EHD can be different.

¹⁾V. S. Bagaev, L. V. Keldysh, N. N. Sibel'din, and V. A. Tsvetkov, Zh. Eksp. Teor. Fiz. 70, 702 (1976) [Sov. Phys. JETP 43, 362 (1976)]; Preprint Fiz. Inst. Akad. Nauk No. 117, 1975.

²⁾L. V. Keldysh, Pis'ma Zh. Eksp. Teor. Fiz. 23, 100 (1976)

- [JETP Lett. **23**, 86 (1976)]; Preprint Fiz. Inst. Akad. Nauk No. 178, 1975.
- ³T. A. Astemirov, V. S. Bagaev, L. I. Paduchikh, and A. G. Poyarkov, Pis'ma Zh. Eksp. Teor. Fiz. **24**, 225 (1976) [JETP Lett. **24**, 200 (1976)].
- ⁴T. A. Astemirov, V. S. Bagaev, L. I. Paduchikh, and A. G. Poyarkov, Fiz. Tverd. Tela (Leningrad) **19**, 937 (1977) [Sov. Phys. Solid State **19**, 547 (1977)].
- ⁵B. M. Ashkinadze and I. M. Fishman, Fiz. Tekh. Poluprovodn. **11**, 301 (1977) [Sov. Phys. Semicond. **11**, 174 (1977)].
- ⁶T. C. Damen and J. M. Worlock, Proc. Third Intern. Conf. on Light Scattering on Solids, Campinas, Brazil, 1975, p. 183; J. M. Worlock, Proc. First Soviet-American Symposium on Theory of Light Scattering in Solids, Moscow, 1975, p. 195.
- ⁷M. Combescot, Phys. Rev. B **12**, 1591 (1975).
- ⁸A. D. Durandin, N. N. Sibel'din, V. B. Stopachinskiĭ, and V. A. Tsvetkov, Pis'ma Zh. Eksp. Teor. Fiz. **26**, 395 (1977) [JETP Lett. **26**, 272 (1977)].
- ⁹V. V. Katyryn, N. N. Sibel'din, V. B. Stopachinskiĭ, and V. A. Tsvetkov, Fiz. Tverd. Tela (Leningrad) **20**, No. 5 (1978) [Sov. Phys. Solid State **20**, No. 5 (1978)].
- ¹⁰J. C. Hensel, T. G. Phillips, and T. M. Rice, Phys. Rev. Lett. **30**, 227 (1973).
- ¹¹R. M. Westervelt, T. K. Lo, J. L. Staehli, and C. D. Jeffries, Phys. Rev. Lett. **32**, 1051 (1974).
- ¹²C. Benoit à la Guillaume, M. Capizzi, B. Etienne, and M. Voos, Solid State Commun. **15**, 1031 (1974).
- ¹³T. A. Astemirov, V. S. Bagaev, L. I. Paduchikh, and A. G. Poyarkov, Kratk. Soobshch. Fiz. No. 11, 3 (1976).
- ¹⁴B. M. Ashkinadze and I. M. Fishman, Fiz. Tekh. Poluprovodn. **11**, 408 (1977) [Sov. Phys. Semicond. **11**, 235 (1977)].
- ¹⁵P. S. Gladkov, B. G. Zhurkin, and N. A. Penin, Fiz. Tekh. Poluprovodn. **6**, 1919 (1972) [Sov. Phys. Semicond. **6**, 1649 (1973)].
- ¹⁶B. M. Ashkinadze, N. N. Zinov'ev, and I. M. Fishman, Zh. Eksp. Teor. Fiz. **70**, 678 (1976) [Sov. Phys. JETP **43**, 349 (1976)].
- ¹⁷L. D. Landau and E. M. Lifshitz, Élektrodinamika sploshnykh sred (Electrodynamics of Continuous Media), Fizmatgiz, 1959, §84. [Pergamon, New York, (or Oxford, 1968)].
- ¹⁸V. S. Bagaev, N. V. Zamkovets, L. V. Keldysh, N. N. Sibel'din, and V. A. Tsvetkov, Zh. Eksp. Teor. Fiz. **70**, 1501 (1976) [Sov. Phys. JETP **43**, 783 (1976)]; Preprint Fiz. Inst. Akad. Nauk No. 139, 1975.
- ¹⁹J. L. Staehli, Phys. Status Solidi B **75**, 451 (1976).
- ²⁰R. M. Westervelt, Phys. Status Solidi B **74**, 727 (1976).
- ²¹V. A. Zayats, V. N. Murzin, I. N. Salganik, and K. S. Shifrin, Zh. Eksp. Teor. Fiz. **73**, 1422 (1977) [Sov. Phys. JETP **46**, (1977)]; Preprint Fiz. Inst. Akad. Nauk No. 38, 1977.

Translated by J. G. Adashko

Damping of sound in antiferromagnets of the easy-plane type with a high Néel temperature

V. S. Lutovinov, V. L. Preobrazhenskii, and S. P. Semin

Moscow Institute of Radiotechnology, Electronics, and Automation

(Submitted 5 October 1977)

Zh. Eksp. Teor. Fiz. **74**, 1159-1169 (March 1978)

The effect of the magnon system on the damping of sound is considered for high-temperature ($T_N > \Theta_D$) antiferromagnets with anisotropy of the "easy plane" type. It is shown that over a broad frequency range, the damping is determined by exchange-amplified relativistic phonon-magnon interaction. The damping of ultrasound has a peculiar frequency, temperature, and field dependence; in the hypersound range, the coupling of the magnetic and elastic subsystems leads to a peak in the frequency dependence of the damping. The calculation is carried out by the diagram method. The applicability of the phenomenological approach to the calculation of the relaxation times of coupled magnetoelastic waves is discussed.

PACS numbers: 71.36.+c

INTRODUCTION

As is well known, damping of sound in dielectrics is caused by interaction of it with thermal phonons by virtue of the anharmonicity of the oscillations of the crystal lattice.^[1,2] In magnetic dielectrics, the damping of sound may be determined by interaction with magnons.^[3-5] The magnon subsystem plays an especially important role in shaping the acoustic properties of high-temperature antiferromagnets with anisotropy of the "easy plane" type (AFEP), such as α -Fe₂O₃ and FeBO₃, because the magnetoelastic coupling of relativistic nature in AFEP is significantly amplified by intersublattice exchange interaction.^[6] In relatively weak magnetic fields H (for α -Fe₂O₃, when $H \leq 1$ kOe), the coupling is so strong that the experimentally observed magnetic corrections to the second-order dynamic moduli of elasticity amount to tens of percent.^[7,8] The strong mixing of phonons with magnons that occurs in

AFEP, even in the absence of an intersection of the acoustic and spin-wave spectra, renders significant some channels for relaxation of phonons that do not, as a rule, play a role in ferromagnets. In particular, the nonlinearity of the magnetic subsystem and the magnetoelastic coupling introduce into the elastic subsystem of AFEP an additional anharmonicity that may significantly exceed the elastic anharmonicity of ordinary solids.^[9]

In the analysis of sound damping, one usually distinguishes two characteristic cases, corresponding to different relations between the frequency of the sound wave being considered, Ω , and the mean lifetime τ of the intermediate states that take part in the relaxation process. When $\Omega\tau \gg 1$, the finiteness of the lifetime of the intermediate states is, as a rule, unimportant, and the sound damping can be calculated, for example, by the usual quantum-mechanical formula for the transi-